N84 10146 D2

# TRENDS IN SHUTTLE ENTRY HEATING FROM THE CORRELATION OF FLIGHT TEST MANEUVERS

James K. Hodge
Air Force Institute of Technology
Wright-Patterson Air Force Base, Ohio

## SUMMARY

A new technique was developed to systematically expand the aerothermodynamic envelope of the Space Shuttle Thermal Protection System (TPS). The technique required transient flight test maneuvers which were performed on the second, fourth, and fifth Shuttle reentries. Kalman filtering and parameter estimation were used for the reduction of embedded thermocouple data to obtain best estimates of aerothermal parameters. Difficulties in reducing the data were overcome or minimized. Thermal parameters were estimated to minimize uncertainties, and heating rate parameters were estimated to correlate with angle of attack, sideslip, deflection angle, and Reynolds number changes. Heating trends from the maneuvers allow for rapid and safe envelope expansion needed for future missions, except for some local areas.

## INTRODUCTION

Because of the lifting capability of the Space Shuttle orbiter, its ranging capability and the aerodynamic heating to its TPS can vary significantly with attitude and in turn with the reentry trajectory. Flight simulators for most airplanes today have fairly standardized equations of motion in terms of linearized stability and control derivatives for example. No such capability existed for aerodynamic heating. Development of a standardized procedure on flight simulators was and is needed for manned reentry vehicles.

Most heat transfer data from wind tunnel tests for the orbiter were fairly standardized. The ratio of film transfer coefficient to a reference stagnation coefficient was tabulated as a function of angle of attack, sideslip, deflection angle, and Reynolds number. The wind tunnel data must be scaled to flight conditions, however, especially when the flow in the wind tunnel was transitional. Various theories to accomplish this were often buried in large programs which primarily output temperature time histories and were not appropriate for flight simulators or for mission planning. A simplified method (Ref. 1-2) was used for mission planning and was adapted and modified for flight simulators (Ref. 3-5). A one-dimensional thermal model was used to improve accuracy for bondline temperatures, and simplified heating ratios were modified to a tabulated form similar to the wind tunnel ratios, or scaled ratios could be used. An added advantage of this approach was flexibility for updating from flight test data.

A systems approach was used to develop the new technique for aerothermodynamic envelope expansion of the orbiter for operational missions at Vandenburg Air Force Base. A diagram of the approach is summarized by Figure 1. The systems approach essentially addresses operational needs for the life of the vehicle and not just

needs for the next flight. Once the vehicle design was frozen, wind tunnel data and theory established a simulator data base for heating ratios. Tabulated heating ratios and a one-dimensional thermal model for several control points (Ref. 6) were programmed on the simulator at the Air Force Flight Test Center (AFFTC) to obtain both surface and bondline temperatures. Using the thermal model also allowed calculation of temperatures which would be measured by existing thermocouples in the TPS. Thus, not only were temperatures on future operational flights predicted, but thermocouple response during transient flight test maneuvers was also simulated. The data reduction technique for heating estimation, referred to as HEATEST, was developed to estimate heating parameters in a manner similar to estimation of stability and control derivatives during aerodynamic flight test maneuvers. Pushover-pullup (POPU) maneuvers and flap maneuvers caused sufficient thermocouple response to allow aerothermodynamic envelope expansion. The POPU allowed angle of attack envelope expansion (heating as a function of angle of attack) needed for more cross range. Flap maneuvers allowed axial center of gravity expansion (heating as a function of elevon and flap deflection.). Lateral center of gravity expansion (heating as a function of sideslip) could not be accomplished by maneuvers. By addressing the overall need for flexible and quick updating of the simulator data base, almost identical equations for the thermal model and heating rates were used in the data reduction program.

The data reduction program actually became a data correlation program when thermocouple data from flight test maneuvers were input. Maneuvers were designed to vary angle of attack, for example, while other variables were nearly constant. The heating rate at a given angle of attack was assumed to be the same, and thus to correlate. Otherwise, any hysteresis during a manuever would be due to error in the thermal model. Uncertainty was thus decreased by identifying this error by estimating thermal model parameters. Use of a Kalman filter further minimized other uncertainties due to modeling. Details of the technique are given in References 3,4,5, and 7.

Lessons have been learned by applying this new technique to thermocouple data from flight test maneuvers on the second and fourth Space Transportation Systems flights (STS-2 and STS-4). Another maneuver is also available from STS-5. Real-gas effects, internal radiative and convective cooling, and late transition are among heating trends which have been identified from thermocouple data, but only trends from transient flight test maneuvers will be emphasized in this paper.

## THERMOCOUPLE INSTRUMENTATION

The excellent thermocouple instrumentation embedded in the orbiter TPS was designed for typical reentry profiles, and not for transient flight test maneuvers. For future vehicles, considerations for flight test maneuvers should be emphasized.

Surface thermocouples were installed in the TPS and covered with a thin coating of thickness $\Delta X_A$. This coating was applied by hand and according to weight, not thickness. For a transient maneuver, error in the coating thickness can cause large uncertainty in the heating rate. Error in the specific heat and conductivity of the coating could also cause more uncertainty. Therefore, an effective coating thickness (equivalent to the surface thermocouple depth and including any significant wire heat capacity) was estimated during flight test maneuvers by the HEATEST program.

The coating thickness of High-temperature Reusable Surface Insulation (HRSI)

was expected to be between 10 to 15 mils (0.025 to 0.04 cm). Estimates for coating thickness on HRSI have varied between a maximum of 21 mils (0.05 cm) at an outboard elevon location (V07T9730) to 15 mils at a lower surface location (V09T9527).

Nomex felt Flexible Resuable Surface Insulation (FRSI) coating was expected to be around 7 mils (0.02 cm). A location on the side of the Orbital Maneuvering System (OMS) pods were of primary concern because of discoloration of the FRSI during the first flight (STS-1). Because of the discoloration, the FRSI was apparently coated again, increasing the coating thickness. An estimate for the FRSI coating during the Mach 20 POPU on STS-2 was 20 mils (0.05 cm) at one location (V07T9976). However, a time skew of 3 seconds was also necessary for data correlation.

Time skews were identified as a serious problem based on estimates from simulated thermocouple data in Ref. 3. If thermocouple samples incorrectly led samples of the angle of attack by only one second, for example, estimates for the HRSI coating thickness became negative and physically unrealistic. If the thermocouple lagged by a second, then the estimates for coating thickness increased. Since the thermocouple and angle of attack were recorded on different recorders with no common clock, there was and is a concern over time skews. The actual sample time was also unknown within the sampling rate, which was once per second for thermocouples and angle of attack.

Thermocouples were not calibrated before the first flights. Most of the error associated with a calibration would probably only be in the form of a bias since calibration curves for thermocouples are well known. Most bias errors could be checked at ambient conditions inside the hangar within the data recorder resolution, which for the orbiter was an eight-bit word. This resolution was the primary noise source for the reduction of orbiter thermocouple data during transient maneuvers. Each thermocouple was scaled according to the anticipated maximum temperature at its location to minimize the resolution error. Calibration curves were then approximated by polynomials and an additional small error was introduced.

It is suggested that thermocouple installation on future vehicles with a low-conductivity thermal protection system be similar to the orbiter with the following improvements. A pressure transducer, surface thermocouple, and bondline thermocouple should be at the same location to enhance utilization of all measurements. A step input to the installed thermocouples with a known heat source should be used to verify the thermal model (at least at ambient conditions). The timing of the step input relative to the thermocouple samples is crucial to accurate estimation of the effective coating thickness. An accurate calibration curve could be practically used if all thermocouples of the same type are scaled identically and higher data resolution is used. Raw-data reduction would be simplified at the expense of more data storage capability. Real-time data links could possibly offset the additional data storage. In addition, fewer thermocouples may be necessary because of a better understanding of reentry heating gained from the thermocouple measurements on the orbiter. More flexibility in installing thermocouples at critical locations, which may not be identified until after a first flight, could also reduce the number of measurements. Although a higher sample rate is needed during flight test maneuvers, a lower sample rate may be sufficient for most of the reentry.

## THERMOCOUPLE DATA REDUCTION

The reduction of thermocouple data using the HEATEST program was first success-

fully demonstrated by simulating thermocouple data on a typical lower surface location (Ref. 3). Thermocouple data on HRSI during a transient maneuver in a wind tunnel test was also reduced (Ref. 3, 4, and 5), but difficulty in estimating coating thickness was encountered. Thermocouple data from STS-1 were reduced in References 3 and 7, although data were lost above Mach 14 and there were no maneuvers. Thermocouple data from STS-2 and STS-4 have also been reduced (Ref. 4-6). The data reduction technique and the lessons learned concerning the technique are discussed.

The heating equations and one-dimensional model are referred to as the heating model and thermal model. These models were chosen to be nearly identical to the simulator equations. The ratio (denoted by a bar) of the heating rate (q) or film transfer coefficient (h) to an appropriate reference condition was assumed to be a linear function of the form

$$\bar{q} = \bar{q}_o + \bar{q}_\alpha (\alpha-\alpha_o) + \bar{q}_\beta (\beta-\beta_o) + \bar{q}_{\log RE} (\log RE - \log RE_o) + \bar{q}_{\delta e} (\delta e - \delta eo) + \bar{q}_{\delta bf} (\delta_{bf} - \delta_{bfo}) \quad (1)$$

where $\bar{q}_o$ is the magnitude or intercept at the reference conditions specified by the zero subscript on each variable. The subscripts on the heating ratio ($\bar{q}$) represent partial derivatives with respect to each variable. The variables are angle of attack ($\alpha$), sideslip ($\beta$), logarithm of the freestream Reynolds number (log RE), elevon deflection angle ($\delta e$), and flap deflections ($\delta_{bf}$). Second-order terms with second-derivative parameters were also added sometimes to account for nonlinearity. The heating model in the simulator was analogous to the linear equation when the heating parameters $\bar{q}_o$, $\bar{q}_\alpha$, $\bar{q}_\beta$, $\bar{q}_{\log RE}$, $\bar{q}_{\delta e}$, and $\bar{q}_{\delta bf}$ are functions of the appropriate variables. For data reduction during maneuvers, these parameters were assumed to be constant for short time durations, but to vary during the reentry. The heating rate was obtained by multiplying the ratio by the reference heating ($q_r$). The heating rate was input to the one-dimensional thermal model. A typical TPS cross section for Reusable Surface Insulation (RSI) is shown in Figure 2. The thermal-model equations were solved by the same finite-element (or finite-diffference) method as on the simulator and require initial conditions.

A simplified diagram of the HEATEST algorithm is shown in Figure 3. The MODEL block was identical to the simulator model except the sensitivity and covariance of the temperature at each node were also propagated in time. Initial conditions in the IC block were required for temperature (U), the sensitivity ($U_{\partial K}$) of the temperature to each parameter ($\theta_K$), and the covariance (P) of the temperature. The parameters ($\theta_K$) include both thermal and heating model parameters. The propagated or predicted temperature, sensitivity, and covariance are referred to as a priori values and are denoted by a minus superscript.

If a thermocouple measurement was available, then the a priori temperature was compared with the measured temperature in a Kalman filter algorithm (Ref. 3, 4, 5, and 7) which is referred to as a KALMAN UPDATE. Depending on the Kalman filter tuning (i.e., the uncertainty in the measurement and models), the a priori values were updated to a posteriori values which were donoted by a plus superscript. This process was repeated in a TIME LOOP until the end of a given time segment.

A Newton-Ralphson algorithm was then used to update heating and thermal parameters in the PARAMETER UPDATE block to satisfy a maximum likelihood function for each parameter (Ref. 3, 4, 5, and 7). With the updated parameter, the TIME LOOP

was repeated. This process was repeated for a fixed number of iterations.

## FLIGHT DATA REDUCTION

The HEATEST algorithm was applied to flight thermocouple data. Some difficulty was encountered due to data loss, initial condition generation, and excessive computer time.

Onboard thermocouple data were lost on STS-1 and STS-4, and only telemetry data were obtained. Therefore, the only flights with maneuvers and with thermocouple data are STS-2 and STS-5. Data from STS-5 were not available in time for this paper, but do not appear to change any results. Pressure measurements were lost in STS-2. Therefore, predicted pressures were used for determining RSI conductivity. Telemetry data from STS-4 partially covered both FOPU maneuvers, but caused concern for initial conditions.

Errors in initial conditions were determined to be a source of error in heating parameter estimates based on studies with simulated thermocouple data (Ref. 3). For STS-2, initial conditions were generated by reducing all thermocouple data from entry interface to just prior to the maneuvers at approximately Mach 21. Initially, the on-board dynamic pressure and velocity were used to calculate density. When the pitch jets fired at low dynamic pressure, a large spike was caused in the dynamic pressure and thus in density. HEATEST estimated large angle of attack derivatives since no input variables except angle of attack were changing. If the pitch jets were input and the heating allowed to correlate with this variable, then the program should identify the error. Time segment size was increased instead. The initial conditions for STS-2 maneuvers should therefore be accurate, but excessive computer time was required.

Several methods to decrease the computer time were implemented. Most of the time was used to propagate the covariance. First an adiabatic wall type boundary condition was assumed only for the covariance at a few nodes from the surface. Another approximate initial condition generation procedure was based on a circuit analogy with an empirically determined time constant (Ref. 4-5). Finally, old inefficient library routines were replaced by new more efficient routines (Ref. 8). Analysis of the Mach-20 POPU at a lower surface location (V09T0527-V07T9531) with 14 nodes required 440 seconds on a Cyber 74. The new routines decreased the time to 44 seconds. Using the adiabatic wall assumption would decrease this further but would not allow the use of all in-depth thermocouples. Approximate initial conditions were generated 50 seconds prior to the maneuver and HEATEST was used for initial conditions for the POPU. The behavior of the Kalman filter at each measurement node was demonstrated as shown in Figure 4.

## TRENDS FROM FLIGHT TEST MANEUVERS

Heating and thermal parameters were estimated during maneuvers. Estimates for effective coating thickness have already been discussed. Heating trends from these maneuvers were obtained at a few locations and are presented at a point representative of the lower surface, the elevon control surface and OMS pods on the upper surface.

## Lower Surface

Because of the data loss on STS-4, a lower-surface location (V09T9527-V07T9531) with five embedded thermocouples was investigated. Time histories of the surface thermocouple and angle of attack of the Mach 20 POPU during STS-2 are shown in Figure 5. Time histories of the Mach 12 and 8 POPU during STS-4 are shown in Figures 6 and 7. Note that the pullup portion of the Mach 12 maneuver was unusually long and that telemetry data started during the pushover. Note that the Mach 8 maneuver was short duration.

Results for the Mach 20 maneuver agreed well with wind tunnel data as shown in Figure 8. The trend in angle of attack agrees well and demonstrates that the linear assumption in angle of attack was valid.

The angle of attack heating derivative was lower at Mach 12. This could be a Mach effect or initial condition error caused by the data loss and transition to fully turbulent flow above 44 degrees angle of attack. As seen in Figure 6, the temperature was higher than the simulated temperature based on laminar heating rates. In addition, as suggested by Hertzler (Ref. 6), the axial accelerometer measurement (axial drag) increased discretely for angles of attack above 44 degrees, typical of flow transition, and decreased back to laminar flow below 44 degrees. Thus, sensitivity of transition to angle of attack was demonstrated.

The flow was fully turbulent during the Mach 8 POPU. The higher heating magnitude and larger uncertainty bound are shown in Figure 7. The higher uncertainty was due to the short duration maneuver and perhaps to heating changes with Reynolds number. A Reynolds number derivative could not be estimated even when the angle of attack derivative was fixed. An alternate procedure used sequential five second time segments. The trend in Reynolds number, assuming the angle of attack trend was correct, is shown in figure 9.

## Elevon Control Surface

Heating trends were sucessfully estimated at a location near the tip of the outboard elevon (V07T9730) for numerous maneuvers during STS-2. Time histories are shown for the Mach 21 flap maneuver and Mach 20 POPU in Figure 10. Because there was no thermocouple response, the flap maneuver at Mach 16 is not shown. The Mach 12 flap maneuver is shown in Figure 11.

Nonlinear heating trends in elevon deflection angle were evident as shown in Figure 12 for the Mach 21 maneuver. A second-order polynomial in elevon deflection was used. The cause of the increased heating above five degrees elevon deflection is unknown but could be due to a localized flow phenomenon or to transition to turbulent flow. There is a possibility that a local separation bubble would cause the hypersonic buffet reported on STS-4 when the elevon schedule was five degrees. Because there was no thermocouple response during the Mach 16 maneuver, the elevon heating derivative was zero. This result implies that the heating estimates at Mach 21 are more nonlinear.

Results from the Mach 12 flap maneuver for fully turbulent flow on the elevon are also shown in Figure 12. The data correlated poorly for negative deflection angles. A localized phenomenon or transitional flow at small deflections could cause this behavior. For envelope expansion, the trends at the larger deflection

angles were of primary concern. The lower elevon heating allowed for a trade-off with the flap control surface.

Heating on the flap was lower than expected for a given deflection angle, but because of a shift in the basic pitching moment, larger flap or elevon deflections were required. The heating on the flap changed dramatically with flap deflection, angle of attack, and elevon deflection during STS-2 maneuvers. There was also a Reynolds number trend which made data correlation very difficult (Ref. 9).

## Orbital Maneuvering System Pods

The primary concern for angle of attack envelope expansion was the upper surface, especially the OMS pods. Time histories for the Mach 20 POPU during STS-2 are shown in Figure 13. A large unexpected response occurred on the side of the OMS pod (V07T9976). Although a three-second time skew was necessary, the results from parameter estimates correlate well as shown in Figure 14. The flow impingement on the pod started at 37 degrees angle of attack instead of at 30 degrees as in the wind tunnel. In addition, estimates in Ref. 6 from STS-4 indicate less dependence on Reynolds number than in the wind tunnel. Visual inspection of FRSI discoloration as shown in Fig. 15 indicated a different pattern than expected based on predictions from wind tunnel data.

Investigation of transient maneuvers in the wind tunnel in Ref. 10 to estimate coating thickness demonstrated a similarity with the OMS pod heating. A three-second lag in the thermocouple response was found. A theoretical investigation in Ref. 11 of the lower heating magnitude reported in Ref. 3-5 confirmed the sensitivity of the heating to a discontinuity in wall temperature (or nonisothermal wall caused by an interface between different materials). The stainless-steel leading edge and FRSI test article on a flat plate in the wind tunnel had a step increase in wall temperature. On the OMS pod, there was a step decrease at the low-temperature RSI and FRSI interface as shown in Fig. 15. Therefore, the three-second time skew and some of the increased heating on the OMS pods may be attributed to the nonisothermal wall.

Numerous locations on the Orbiter have an interface between different materials and probably have the same nonisothermal-wall problem. One such local area would be the nose cap and HRSI interface where tiles have slumped due to increased heating as shown in Fig. 16. According to Ref. 11, such an interface near the leading edge would have a rapid recovery. The nose cap surface temperature peaks around Mach 18 corresponding to a POPU on STS-5. The nonisothermal wall effect would be largest at Mach 18. This effect should be considered when heating data is correlated and also for future designs.

## REFERENCES


1. Evans, M.E.: Thermal Boundaries Analysis Program Document. NASA CR-151025, April 1975.

2. Space Shuttle Orbiter Entry Aerodynamic Heating Data Book. Rockwell International Space Division Document Number SD73-SH-0814 C Revision, Books 1 and 2, October 1978.

3. Hodge, J.K., Phillips, P.W., and Audley, D.R.: Flight Testing a Manned Lifting Reentry Vehicle (Space Shuttle) for Aerothermodynamic Performance. AIAA Paper 81-2421, November 1981.

4. Hodge, J.K., Audley, D.R., Phillips, P.W., and Hertzler, E.K.: Aerothermodynamic Flight Envelope Expansion for a Manned Lifting Reentry Vehicle (Space Shuttle). Paper 3-A, AGARD CP-339, October 1982.

5. Hodge, J.K., and Audley D.R.: Aerothermodynamic Parameter Estimation from Space Shuttle Thermocouple Data During Transient Flight Test Maneuvers. AIAA Paper 83-0482, January 1983.

6. Hertzler, E.K. and Phillips, P.W.: Flight Test Derived Heating Math Models for Critical Locations on the Orbiter during Reentry. Shuttle Performance: Lessons Learned, NASA CP-2283, Part 2, 1983, pp. 703-718.

7. Audley, D.R., and Hodge, J.K.: Identifying the Aerothermodynamic Environment of the Space Shuttle Orbiter, Columbia. 6th IFAC Symposium on Identification and System Parameter Estimation, June 1982.

8. Sagstetter, P.W.: Numerical Computation of the Matrix Riccati Equation for Heat Propagation During Space Shuttle Reentry. Master's Thesis, AFIT/GCS/MA/82D-7, Air Force Institute of Technology, Wright-Patterson AFB, Ohio.

9. Wood, J.R.: Body Flap Heat Transfer Data from Space Shuttle Orbiter Entry Flight Test Maneuvers. Master's Thesis, AFIT/GA/AA/82D-12, Air Force Institut of Technology, Wright-Patterson AFB, Ohio.

10. Woo, Y.K.: Transient Heat-Transfer Measurement Technique in Wind Tunnel and Dat Analysis Technique Using System Identification Theory. Master's Thesis, AFIT/GAE/AA/82D-34, Air Force Institute of Technology, Wright-Patterson AFB, Ohio.

11. Cappelano, P.T.: Heat Transfer/Boundary Layer Investigation of Heating Discrepancies in Wind Tunnel Testing of Orbiter Insulating Articles. Master's Thesis AFIT/GA/AA/82D-3, Air Force Institute of Technology, Wright-Patterson AFB, Ohio.

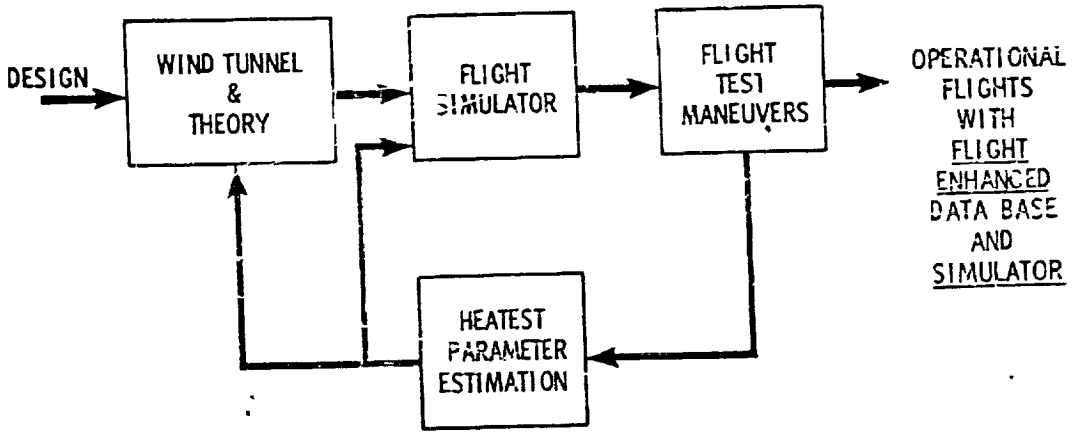


Figure 1.- Systems approach to envelope expansion.

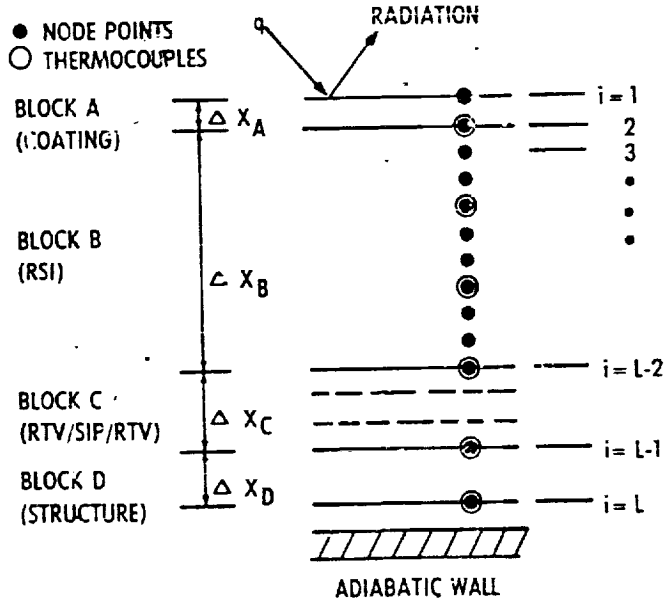


Figure 2.- TPS model cross section.

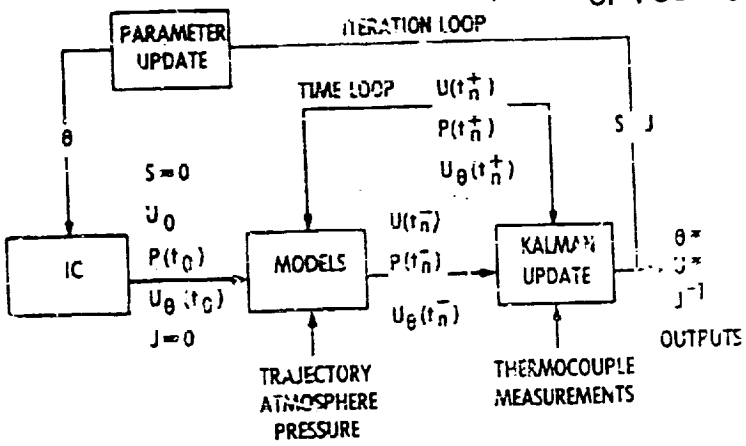


Figure 3.- Simplified HEATEST flow diagram.

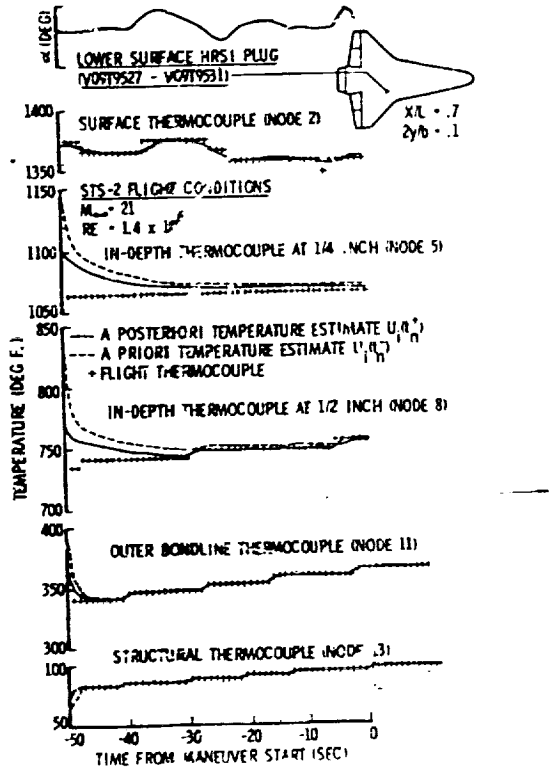


Figure 4.- Comparison of a priori and a posteriori temperature estimates of extended Kalman estimator starting from approximate initial conditions.

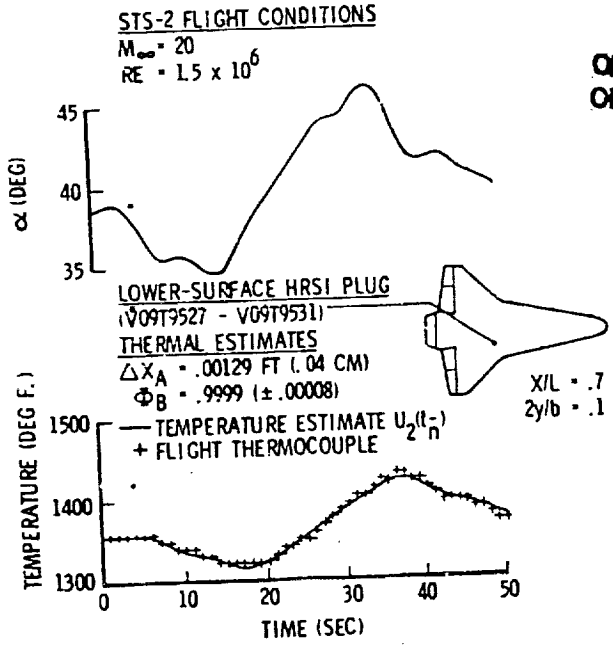


Figure 5.- Lower-surface-plug STS-2 flight thermocouple data (Mach 20 pushover-pullup maneuver).

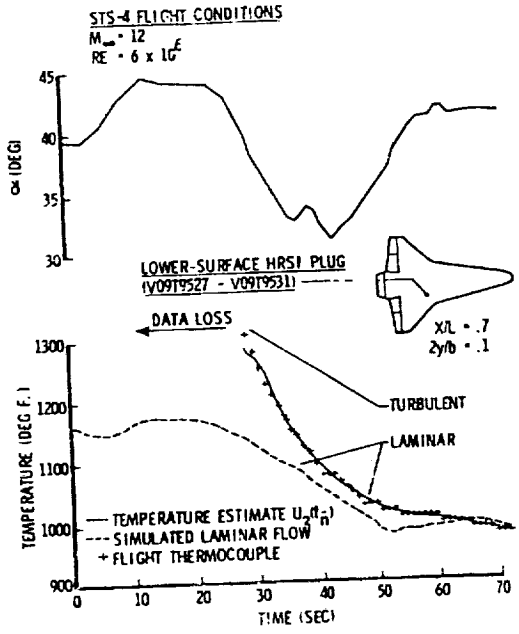


Figure 6.- Lower-surface-plug STS-4 flight thermocouple data with transition onset during Mach 12 pullup-pushover maneuver.

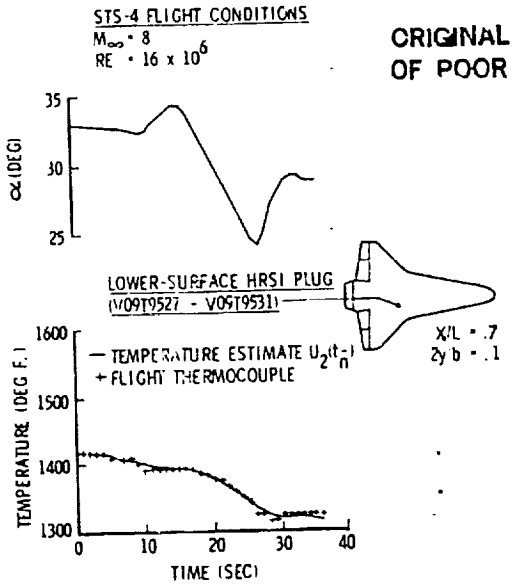


Figure 7.- Lower-surface-plug STS-4 flight thermocouple data for turbulent flow (Mach 8 pullup-pushover maneuver).

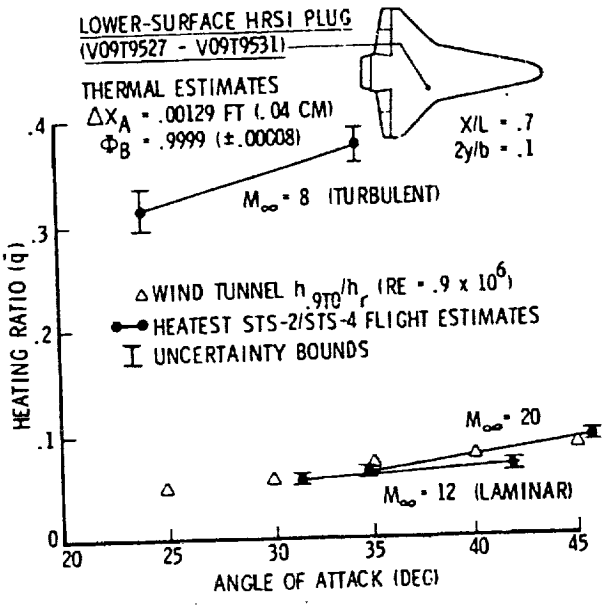


Figure 8.- Heating estimates for lower surface plug from STS-2/STS-4 flight thermocouple data.

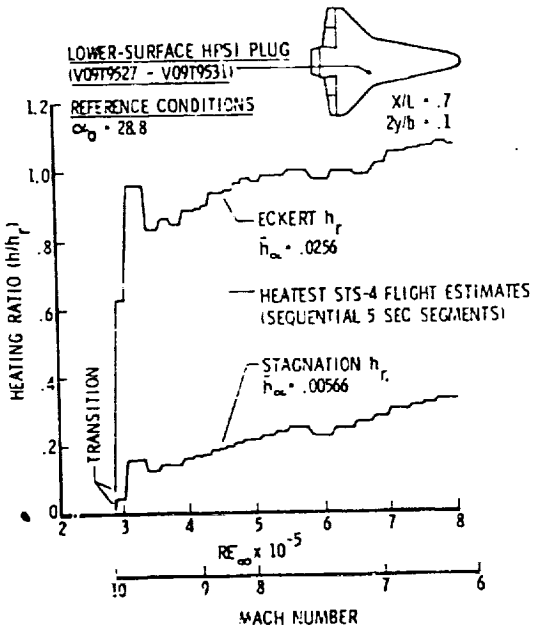


Figure 9.- Heating comparison for STS-4 thermocouple data using both stagnation and Eckert turbulent reference heating to show Reynolds number trends.

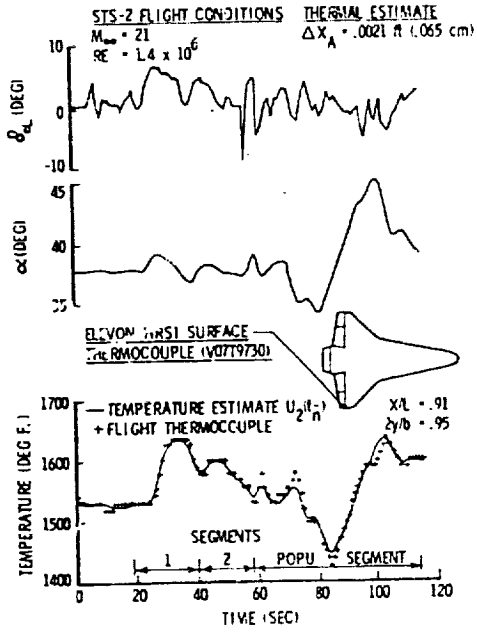


Figure 10.- Outboard elevon STS-2 flight thermocouple data (Mach 21 flap maneuver and Mach 20 pushover-pullup maneuver).

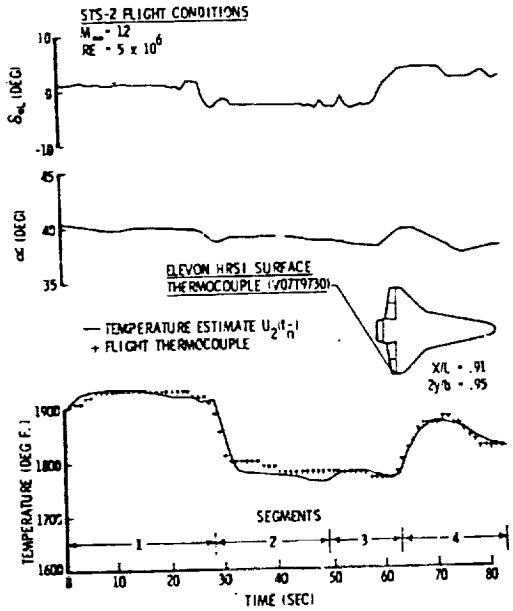


Figure 11.- Outboard elevon STS-2 flight thermocouple data (Mach 12 flap maneuver).

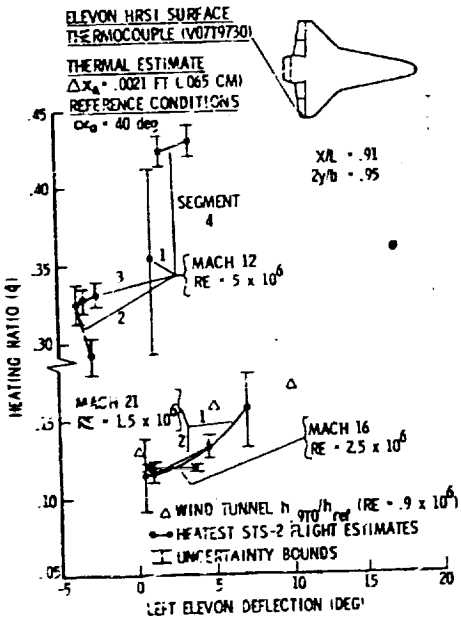


Figure 12.- Heating estimates for outboard elevon from STS-2 flight thermocouple data.

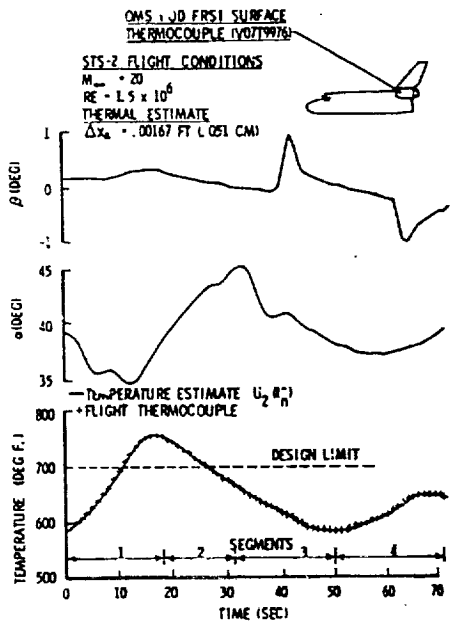


Figure 13.- OMS pod STS-2 flight thermocouple data (Mach 20 pushover-pullup maneuver).

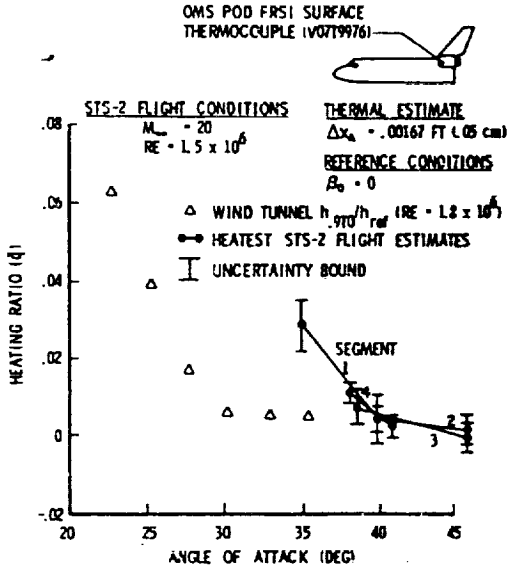


Figure 14.- Heating estimates for OMS pod from STS-2 flight thermocouple data (Mach 20 pushover-pullup maneuver).

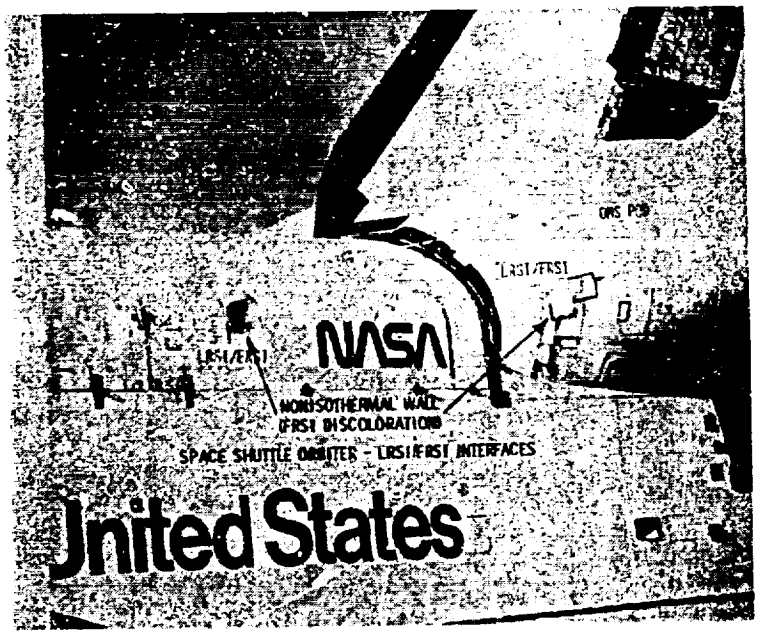


Figure 15.- Space Shuttle orbiter LRSI/FRSI interfaces with a nonisothermal wall and FRSI discoloration.


Figure 16.- Space Shuttle orbiter nose CAP/HRSI interface with a nonisothermal wall and slumped HRSI.